

Studies of Dispersions of (2*S*,6'*R*)-7-Chloro-2',4,6-trimethoxy-6'-methyl-3*H*,4'*H*-spiro[1-benzofuran-2,1'-cyclohex[2]ene]-3,4'-dione in Poly(ethane-1,2-diol)

Jelena Knoblauch[†] and Ingfried Zimmermann^{*‡}

Lehrstuhl für Pharmazeutische Technologie, Julius-Maximilians-Universität Würzburg, Germany, and Institut für Pharmazie und Lebensmittelchemie, Julius-Maximilians-Universität Würzburg, Am Hubland, D-97074 Würzburg, Germany

According to Hess's theorem, the thermodynamics of processes can be described by different routes that have the same start and end points as the original process. Often the energy changes associated with alternative processes can be measured with less uncertainty than the direct process. This is the case for poorly water-soluble drugs where it is hypothesized that the formation of solid solutions might improve drug solubility in water. In a solid solution, the sparingly water-soluble compound is amorphaously dispersed in a highly water-soluble polymeric carrier, for example, poly(ethane-1,2-diol) (PEG) 6000 or 8000. To test this hypothesis, a model drug, (2*S*,6'*R*)-7-chloro-2',4,6-trimethoxy-6'-methyl-3*H*,4'*H*-spiro[1-benzofuran-2,1'-cyclohex[2]ene]-3,4'-dione (griseofulvin), was used that has a low water solubility. The thermodynamic properties of solid dispersions of griseofulvin in PEG 6000 were studied. From the powder X-ray diffraction patterns, we can conclude that solid dispersions of PEG 6000 exist in the form of a 7_2 helix. By means of high-precision calorimetry, the phase diagram of solid dispersions of griseofulvin + PEG 6000 was generated and a PEG + griseofulvin monotectic observed. Unfortunately, no information could be obtained for systems containing a mass fraction less than 0.05 griseofulvin. A quantitative determination of the crystallinity of griseofulvin showed that it exists in its solid dispersions in a completely crystallized form. In addition, we were able to show that an improvement of the water solubility of griseofulvin was achieved by aqueous solutions of PEG without preparation of a melt.

1. Introduction

In a recently published paper,¹ we were able to explain the solubility of (2*S*,6'*R*)-7-chloro-2',4,6-trimethoxy-6'-methyl-3*H*,4'*H*-spiro[1-benzofuran-2,1'-cyclohex[2]ene]-3,4'-dione in water with the Hess theorem as shown in Figure 1.^{2,3}

As can be seen from Figure 1, the dissolution energy is given by the sum of the sublimation energy, of the transfer energy of the sublimated molecules into free volumes formed in the solvent, and eventually of the solvation energy. With poorly soluble drugs, the dissolution energy is rather low. Therefore, its accurate determination may be very difficult. The energies of the alternative routes, however, are significantly higher. Consequently, these can be determined rather precisely or calculated. Comparing the contributions to the dissolution energy permits the determination of methods to improve the solubility of a given compound.

In most cases studied so far, the energy of the endothermic sublimation process is almost as high as the energy of the exothermic solvation, thus limiting the solubility of the compound.

2. Experimental Section

(2*S*,6'*R*)-7-Chloro-2',4,6-trimethoxy-6'-methyl-3*H*,4'*H*-spiro[1-benzofuran-2,1'-cyclohex[2]ene]-3,4'-dione with CAS # 126-07-8 and known commonly as griseofulvin, shown in Figure 2, was used as supplied by the Arzneimittelwerke Dresden, AWD (Dresden, Germany).

* Corresponding author. E-mail: i.zimmermann@pharmazie.uni-wuerzburg.de. Tel.: +49 931-31 85471. Fax: +49 931-31 84606.

[†] Lehrstuhl für Pharmazeutische Technologie.

[‡] Institut für Pharmazie and Lebensmittelchemie.

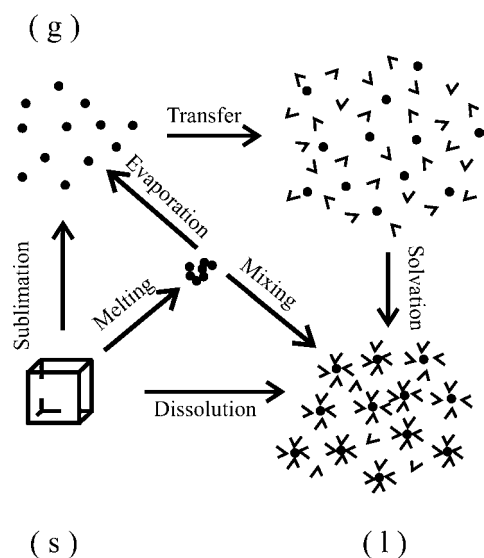


Figure 1. Alternative paths that describe the dissolution process.

The particle dimensions were less than 5 μm . Poly(ethane-1,2-diol) (CAS # 25322-68-3) was purchased from two suppliers. The first batch (Macrogol 6000) was purchased from Merck (Darmstadt, Germany) as a free-flowing white powder and according to the supplier has a molar mass of 6376 $\text{g}\cdot\text{mol}^{-1}$. The second batch (Lutrol 6000) was purchased from BASF SE (Ludwigshafen, Germany) as white flakes with a cited average molar mass of between (5000 and 7000) $\text{g}\cdot\text{mol}^{-1}$. For the determination of the enthalpies of melting and solution, the molar mass must be known, and this was determined by the

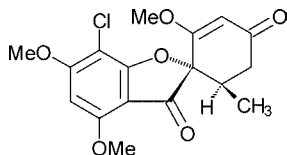


Figure 2. Structure of griseofulvin of molar mass $352.77 \text{ g}\cdot\text{mol}^{-1}$.

Table 1. Molar Mass M and Polydispersity P_D of the Two Batches of Polyethylene Glycol 6000 (PEG 6000)

PEG 6000	\overline{M}_w	\overline{M}_n	P_D
	$\text{g}\cdot\text{mol}^{-1}$	$\text{g}\cdot\text{mol}^{-1}$	
batch 1 (Maldi-TOF, lin.)	6380	5820	1.10
batch 1 (Maldi-TOF, refl.)	5590	4810	1.16
batch 1 (GPC)	7440	6680	1.11
batch 2 (Maldi-TOF, lin.)	6340	6280	1.01
batch 2 (Maldi-TOF, refl.)	6260	6190	1.01
batch 2 (GPC)	6890	6440	1.07

Max-Planck-Institute of polymer research, Mainz (Germany), by mass spectroscopy (Maldi-TOF) and gel permeation chromatography (GPC). The ratio of the weight-average of the molar mass \overline{M}_w to its number-average of the molar mass \overline{M}_n defines the polydispersity of a polymer P_D through

$$P_D = \frac{\overline{M}_w}{\overline{M}_n} \quad (1)$$

The results obtained are listed in Table 1.

The polydispersity of both polymer batches is close to 1 which implies the polymers are characterized by narrow distributions of the molar mass molecular weight. This holds especially for batch 2 (Figure 3).

The distilled water used in the experiments was prepared as described in ref 1, as was the concentration of griseofulvin.

Thermal Analyses. The melting behavior of griseofulvin, of the solid dispersions, and of the physical mixtures of griseofulvin and PEG 6000 was studied by differential thermal analysis (DTA) combined with thermogravimetry (TG) using a Setaram DTA/TG calorimeter TG 92 (Setaram, Caluire, France). The instrument was calibrated using

indium^{4,6,8} with a purity of 0.99999, obtained from Fluka, Buchs, Switzerland. It has an enthalpy of fusion of $(3.283 \pm 0.004) \text{ kJ}\cdot\text{mol}^{-1}$ at a temperature of $156.6 \text{ }^\circ\text{C}$.^{5,7} The enthalpy of fusion ΔH_{fus} and the melting temperature can be obtained directly from the calorimeter.

Calorimetry. The melting temperature of PEG 6000, the direct determinations of the enthalpy of solution, and the sublimation enthalpies were determined with a Setaram calorimeter C80 (Setaram, Caluire, France) that was constructed according to the design reported in ref 4. The sensitivity of this equipment is in the range of $(2 \text{ to } 5) \mu\text{W}$ with a time constant of response of about 200 s. Details of the measurements and method of determining the enthalpy are provided in ref 1.

The crystallinity of griseofulvin contained in solid dispersions as well as the mixtures was studied by X-ray powder diffraction using a Phillips (Hamburg) diffractometer with a vertical goniometry PW 1820/00 and X-rays with the wavelengths of $\text{Cu K}_{\alpha 1} = 1.54060 \cdot 10^{-10} \text{ m}$ and $\text{Cu K}_{\alpha 2} = 1.54439 \cdot 10^{-10} \text{ m}$. The diffraction intensities were obtained by Bragg–Brentano geometry. The sample particle sizes were in the range of $(125 \text{ to } 250) \mu\text{m}$, and the griseofulvin particles were $<5 \mu\text{m}$. The X-ray spectra of pure griseofulvin and PEG 6000 were calculated with the program Powder Cell 1.0.⁹

The degree of crystallinity of griseofulvin in solid dispersions as well as in the mixtures was determined using an external standard.^{10,11} The intensity of a given peak i of a phase α in a mixture was obtained from

$$I_{i,\alpha} = K_{i,\alpha} \cdot \frac{x_\alpha}{\rho_\alpha \cdot \mu_s} \quad (2)$$

where $I_{i,\alpha}$ is the intensity of the peak i of the phase α in a binary mixture; x_α is the mass fraction of the phase α in a binary mixture; ρ_α is the density of the phase α ; μ_s is the mass absorption coefficient; and $K_{i,\alpha}$ is the device specific constant (scale factor of peak i of phase α). The intensity of a peak i of the pure phase α (mass fraction $x_\alpha = 1$) is given by

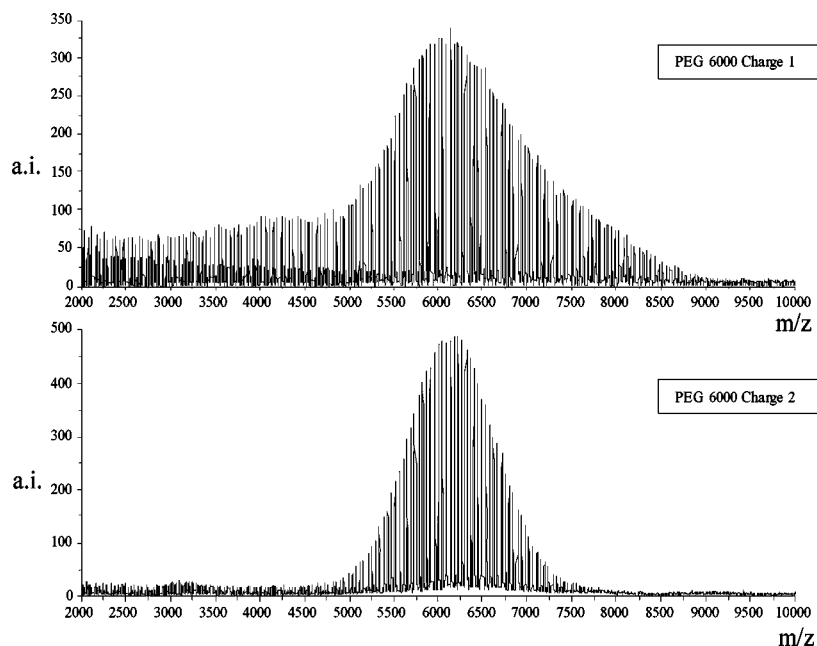


Figure 3. Ratio of molar mass to charge distributions for the two batches of PEG 6000 determined by Maldi-TOF.

$$I_{i,\alpha}^0 = K_{i,\alpha} \cdot \frac{1}{\rho_{\alpha} \cdot \mu_{\alpha}} \quad (3)$$

The mass fraction x_{α} is then given by

$$x_{\alpha} = \frac{I_{i,\alpha} \cdot \mu_s}{I_{i,\alpha}^0 \cdot \mu_{\alpha}} \quad (4)$$

The mass absorption coefficient of the pure phase α is only dependent on the contributions of the atoms defining the molecules of phase α

$$\mu = \sum \omega_i \cdot \mu_i \quad (5)$$

where μ_i is the mass absorption coefficient of the pure phases α and β with mass fraction ω_i of the elements of the type i in the molecules forming the pure phases α and β ($\sum \omega_i = 1$). The mass absorption coefficients of the elements of type i at a given wavelength were obtained from the literature.¹²

The mass absorption coefficient μ_s of a binary mixture is defined by

$$\mu_s = x_{\alpha} \cdot \mu_{\alpha} + x_{\beta} \cdot \mu_{\beta} \quad (6)$$

where $\mu_{\alpha,\beta}$ is the mass absorption coefficient of the pure phases α and β , respectively, and $x_{\alpha,\beta}$ is the mass fraction of the phases α and β , respectively, in the binary mixture. The degree of crystallinity D of griseofulvin (phase α) is obtained from

$$D = \frac{x_{\alpha}}{x_{\alpha,0}} \quad (7)$$

where x_{α} is the mass fraction of griseofulvin obtained from the X-ray diffraction and $x_{\alpha,0}$ is the gravimetrically determined griseofulvin mass fraction. For the determination of the degree of crystallinity of griseofulvin, the X-ray signals at 10.78°, 13.24°, 16.54°, and 28.53° were used.

Preparation of Dispersions of Griseofulvin in PEG. The basic procedure used to produce dispersions of griseofulvin and PEG 6000 was to weigh into a glass vessel and, after sealing, store in a thermostat at a temperature of 67 °C for a time of 1 h during which the sample was stirred every 15 min. After this storage, the vessel containing the melt was transferred into a silicon oil thermostat at a temperature of 10 °C where it was stored for a further 1 h in which the melt solidified. The solidification was completed in a desiccator overnight. The next day the dispersion was ground in a mortar and pestle, and to eliminate the effect of particle size on the thermal analysis, only those between (125 and 250) μm were used. The mixtures had griseofulvin with mass fractions of (3 and 10) %. There were three modifications to this general procedure, and these were as follows: (a) after mixing in a glass vessel the sample was continuously stirred for a time of 60 min at a temperature of 100 °C before continuing with the procedure; (b) method a was followed, and the glass vessel containing the hot dispersion was placed into liquid nitrogen for a time of 30 min; and (c) the procedure followed a, and after continuous stirring at a temperature of 100 °C the dispersion was poured into liquid nitrogen where it solidified into small spheres that were collected when the particle diameter was in the range (125 to 250) μm and stored in a desiccator overnight for subsequent use. The mixtures of griseofulvin and PEG 6000 were prepared from ground PEG 6000 of the desired size mixed with griseofulvin in a Turbula mixer (Type T2C, Fa. Bachofen, Basel, Switzerland) for a time of 10 min.

3. Results and Discussion

The properties of griseofulvin and PEG 6000 were characterized by thermal analyses over the range of conditions experienced, and the results confirmed observations reported in the literature,^{13–18} particularly those of Buckley¹³ and Yang¹⁶ that suggest PEG 6000 exists in both a stretched and a folded form. The polymer, Macrocol 6000, Batch 1, was ground and thermally analyzed and found to have one melting temperature of $t_{\text{max}} = (61.03 \pm 0.01)$ °C that according to Buckley¹³ corresponds to the twice folded form of PEG 6000 shown in Figure 4.

The thermally treated PEG 6000 showed two clearly separated temperatures from thermal analysis of $t_{\text{max}1} = (60.66 \pm 0.06)$ °C and $t_{\text{max}2} = (62.74 \pm 0.05)$ °C with a relatively small response at a temperature of 53.8 °C. According to Buckley¹³ and Craig,¹⁴ the form melting at $t_{\text{max}1}$ corresponds to the folded form of the polymer, whereas the higher melting form, $t_{\text{max}2}$, represents the stretched form. The melting behavior of the PEG 6000 supplied by BASF SE (Lutrol 6000), and labeled as Batch 2, was different from Macrocol 6000, Batch 1, as shown in Figure 5.

The mechanically treated form showed two distinct melting temperatures corresponding to the folded and the stretched

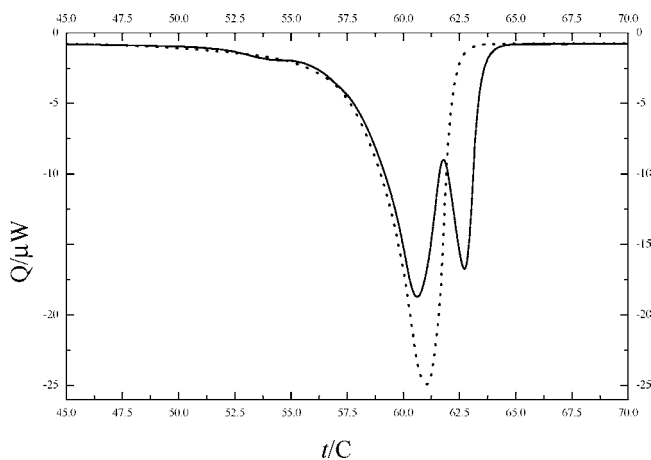


Figure 4. Heat flow Q as a function of temperature t demonstrating the melting behavior of mechanically and thermally treated PEG 6000 from Batch 1 at a heating rate of $0.1 \text{ K} \cdot \text{min}^{-1}$: - - -, mechanically treated; —, thermally treated.

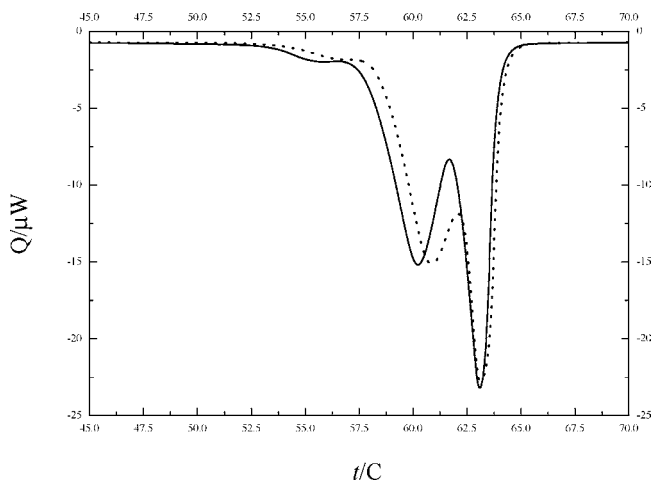


Figure 5. Heat flow Q as a function of temperature t demonstrating the melting behavior of mechanically and thermally treated PEG 6000 from Batch 2 at a heating rate of $0.1 \text{ K} \cdot \text{min}^{-1}$: - - -, mechanically treated; —, thermally treated.

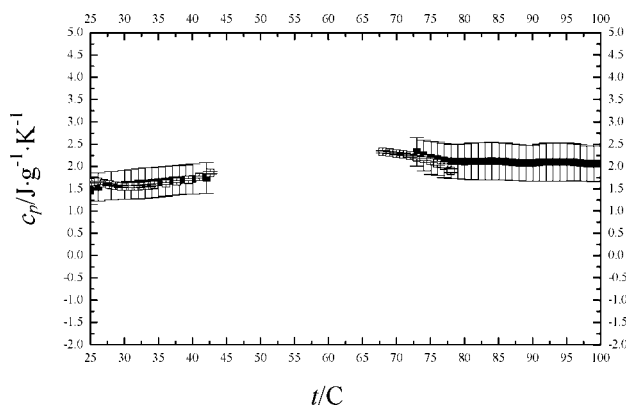


Figure 6. Heat capacities C_p of PEG 6000 in the liquid state purged with nitrogen to prevent degradation as a function of temperature t obtained at two heating rates: ■, $2 \text{ K}\cdot\text{min}^{-1}$; □, $0.1 \text{ K}\cdot\text{min}^{-1}$, air atmosphere with calorimeter C80.

conformations. In Batch 2 the stretched form prevailed, and thermal treatment only minimally changed this situation. However, the shoulder in the temperature range of (53 to 55) °C was more pronounced than with Batch 1. To allow for the calculation of the standard enthalpy, the standard entropy, and the standard Gibbs function of the melting for PEG 6000, the heat capacities of its solid and liquid forms were determined with both calorimeters (Table 3).

In the calorimeter C80, only measurements in air were possible. In the presence of oxygen, a small degradation peak was observed consistent with that reported by Lheritier.¹⁹ As this small peak resulted in relatively large standard deviations, the heat capacities of solid and molten PEG 6000 were also determined in the DSC/TG 92 which permitted use of a nitrogen purge. The results obtained from this experiment are shown in Figure 6.

The agreement of both methods is rather good. The enthalpies of fusion obtained from both calorimeters for both sample batches are listed in Table 2. From the heat capacities determined in a nitrogen atmosphere, the standard energies of fusion as well as its standard entropy were calculated using the formulas provided in ref 1 with the results summarized in Table 4.

The melts of griseofulvin and PEG 6000 were cooled using three different procedures to determine the influence of cooling on PEG 6000, and each sample obtained was thermally characterized by means of a Setaram calorimeter C80. The PEG samples that after melting were cooled to either room temperature or 10 °C showed two melting temperatures, indicating both the folded and stretched forms were obtained. The samples cooled by pouring the melt into

Table 2. Comparison of the Enthalpies of Fusion ΔH_{fus} for the Two Batches of PEG 6000 after Mechanical and Thermal Treatment Illustrating the Results Obtained for Both Forms

	Batch 1 (Macrocol 6000)		Batch 2 (Lutrol 6000)	
	ground polymer	thermally treated	ground polymer	thermally treated
$\Delta H_{\text{fus}}(\text{total})/$ $\text{kJ}\cdot\text{mol}^{-1}$	1138 ± 4	1139 ± 6	1137	1126
$\Delta H_{\text{fus}}(\text{peak 1})/$ $\text{kJ}\cdot\text{mol}^{-1}$	1138 ± 4	844 ± 7	630	617
$\Delta H_{\text{fus}}(\text{peak 2})/$ $\text{kJ}\cdot\text{mol}^{-1}$	---	295 ± 1	507	509
$t_{\text{max1}}/\text{°C}$	61.03 ± 0.05	60.66 ± 0.06	60.23	60.86
$t_{\text{max2}}/\text{°C}$	---	62.74 ± 0.05	63.08	63.12

Table 3. Heat Capacities C_p of PEG 6000 in the Solid and Liquid State

	$C_p(\text{s})$	$C_p(\text{l})$	ΔC_p
	$\text{kJ}\cdot\text{mol}^{-1}\cdot\text{K}^{-1}$	$\text{kJ}\cdot\text{mol}^{-1}\cdot\text{K}^{-1}$	$\text{kJ}\cdot\text{mol}^{-1}\cdot\text{K}^{-1}$
$0.1 \text{ K}\cdot\text{min}^{-1}$ air	10.323 ± 0.549	13.883 ± 0.855	3.560 ± 1.016
$2 \text{ K}\cdot\text{min}^{-1}$ N_2	10.399 ± 0.478	13.526 ± 0.294	3.127 ± 0.561

Table 4. Standard Gibbs Function and Enthalpy and Entropy of Fusion for PEG 6000 at $T = 298.15 \text{ K}$

$\Delta G_{\text{fus}}^0/\text{kJ}\cdot\text{mol}^{-1}$	110.16
$\Delta H_{\text{fus}}^0/\text{kJ}\cdot\text{mol}^{-1}$	1.0179
$\Delta S_{\text{fus}}^0/\text{kJ}\cdot\text{mol}^{-1}\cdot\text{K}^{-1}$	3.0462

liquid nitrogen showed only the peak ($t_{\text{max}} \approx 60 \text{ °C}$) characterizing the folded conformer shown in Figure 7. However, after two days of storage in a desiccator at room temperature the melting peak changed, indicating a partial transition from the pure folded conformer into a mixture of folded and stretched conformers of PEG 6000. This transition clearly indicates that at room temperature PEG 6000 is at least partially in a rubbery state.

From the thermodynamic data obtained for PEG 6000, it is possible to analyze its dissolution process in more detail. According to the Hess theorem, the dissolution can be described as shown in Figure 8.

The standard enthalpy of mixing can be calculated as the difference of the standard dissolution enthalpy and the standard melting enthalpy to give

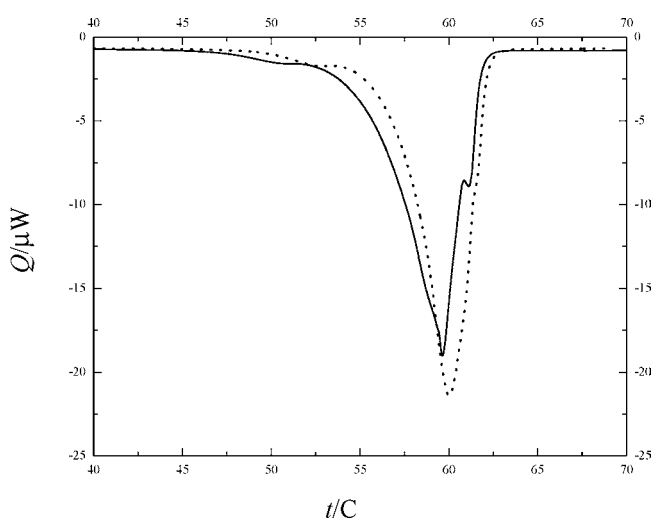


Figure 7. Heat flow Q as a function of temperature t for PEG 6000 cooled in liquid nitrogen immediately after manufacture and after two days storage. ---, cooled in $\text{N}_2(\text{lq})$ immediately after manufacture; — after two days storage.

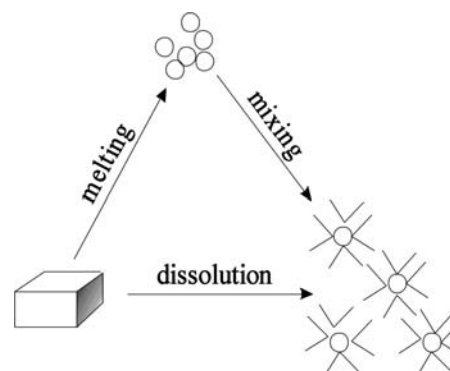


Figure 8. Dissolution processes.

$$\Delta H_{\text{mix}}^{\circ} = \Delta H_{\text{sol}}^{\circ} - \Delta H_{\text{fus}}^{\circ} = (42.8 - 1017.9) \text{ kJ} \cdot \text{mol}^{-1} = -975.1 \text{ kJ} \cdot \text{mol}^{-1} \quad (8)$$

The standard Gibbs function ΔG° of dissolution for PEG 6000 in water was calculated²⁰ from

$$\Delta G^{\circ} = -RT \cdot \ln K \quad (9)$$

where R is the gas constant; $T = 298.15 \text{ K}$; and K is the solubility of PEG 6000 in water. According to Wade et al.,²¹ the water solubility of PEG 6000 at T is $0.341 \text{ mol} \cdot \text{L}^{-1}$ so that $\Delta G^{\circ} = 2.7 \text{ kJ} \cdot \text{mol}^{-1}$ and from

$$\Delta G^{\circ} = \Delta H^{\circ} - T \cdot \Delta S^{\circ} \quad (10)$$

the standard entropy of dissolution for PEG 6000 in water was obtained as $\Delta S^{\circ} = 134.67 \text{ J} \cdot \text{mol}^{-1} \cdot \text{K}^{-1}$. According to the Hess theorem, the formation of solid solutions of griseofulvin in a polymer should increase the former's solubility in water;¹ see Table 5.

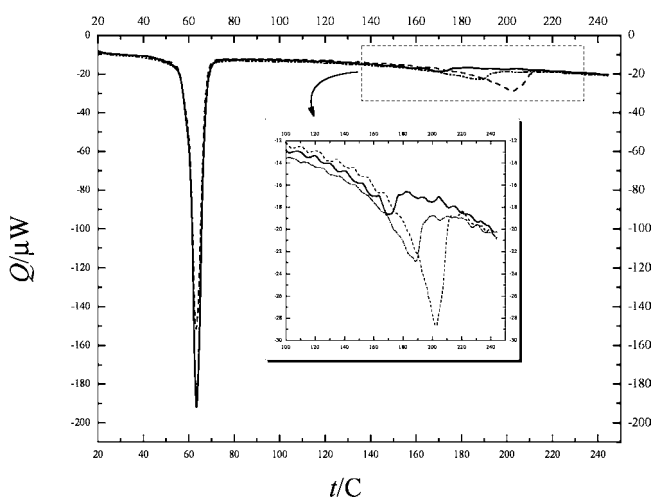


Figure 9. Heat flow Q as a function of temperature t for the melting of solid dispersions containing griseofulvin in PEG 6000. ---, mass fraction of griseofulvin of 0.45; ·····, mass fraction of griseofulvin of 0.3; and —, mass fraction of griseofulvin of 0.2.

Table 5. Standard Enthalpy ΔH , Gibbs Function ΔG , and Entropy ΔS of Dissolution, Melting, and Mixing of Thermally Untreated PEG 6000 in Water

process at 298 K	ΔH°	ΔG°	ΔS°
	$\text{kJ} \cdot \text{mol}^{-1}$	$\text{kJ} \cdot \text{mol}^{-1}$	$\text{kJ} \cdot \text{mol}^{-1} \cdot \text{K}^{-1}$
dissolution	42.8	2.7	0.135
melting	1017.9	110.2	3.046
mixing	-975.1	-107.5	-2.911

Several authors^{22,23} have presented data supporting this hypothesis. However, as described above at room temperature, PEG 6000 is in a rubbery state. This means that diffusion of small molecules within the polymer and hence recrystallization is possible, and consequently, PEG 6000 would not be able to form stable solid solutions.

The melting behavior of systems containing various quantities of griseofulvin prepared according to method c were studied by differential thermal analysis (DTA) at a heating rate of $2 \text{ K} \cdot \text{min}^{-1}$ in a nitrogen atmosphere, and the results are shown in Figure 9.

The griseofulvin could only be detected with DTA when the mass fraction was greater than 0.05. The first peak, shown in Figure 9, corresponds to the melting of PEG 6000, and as expected, the area under this peak decreased with increasing griseofulvin mass fraction. The melting temperature was invariant with the presence of griseofulvin. The second peak was attributed to griseofulvin. DTA diagrams of mixtures of PEG 6000 with griseofulvin were identical with the diagrams shown in Figure 9.

At temperatures above the melting temperature, PEG 6000 decomposes, and this was used to construct the phase diagram of griseofulvin + PEG 6000. The results are listed in Table 6 where, for convenience, the relation between the griseofulvin concentration and the corresponding mole fraction is provided. Figure 10 shows phase diagrams of griseofulvin and PEG 6000. The liquidus line of griseofulvin ends at a mole fraction of 0.5, as the melting energies of griseofulvin in concentrations below 0.05, which corresponds to a mole fraction of 0.49, are too small to be determined by DTA.

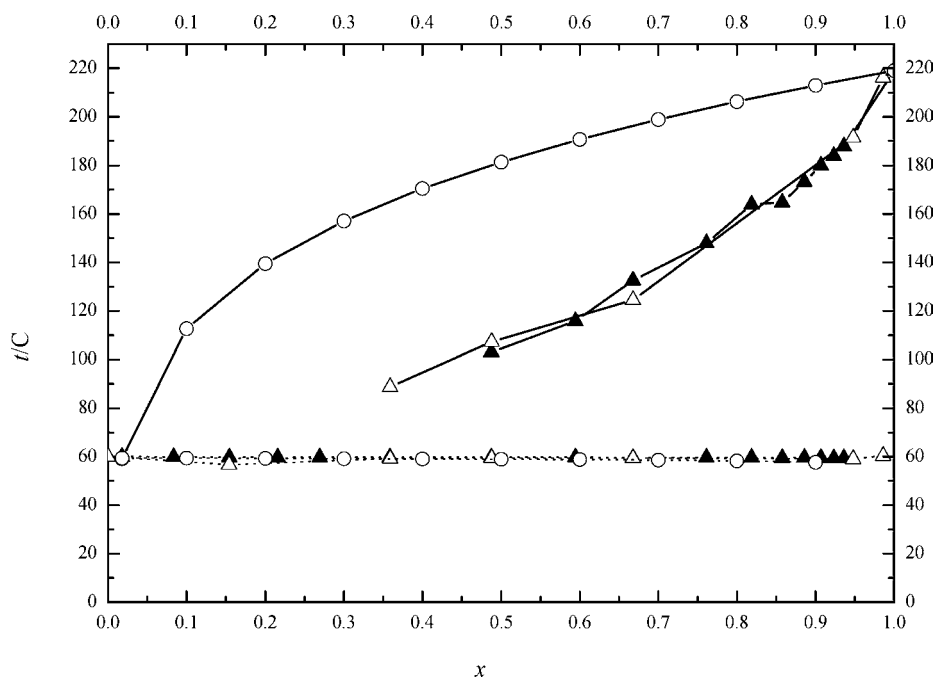


Figure 10. (t, x) phase diagram. \blacktriangle , (griseofulvin(s) + PEG 6000(s)); Δ , (griseofulvin(s) + PEG 6000(l)); \circ , (griseofulvin(l) + PEG 6000(l)).

Table 6. Griseofulvin Mass Fraction w and Mole Fraction x

w	x	w	x
0.001	0.017	0.10	0.667
0.005	0.083	0.15	0.761
0.01	0.154	0.20	0.819
0.015	0.216	0.25	0.858
0.02	0.269	0.30	0.886
0.03	0.359	0.35	0.907
0.05	0.488	0.40	0.923
0.075	0.595	0.45	0.936

The theoretical phase diagram was calculated according to the van't Hoff equation²⁰

$$-\ln x_i = \frac{\Delta H_{\text{fus},i}}{R} \left(\frac{1}{T} - \frac{1}{T_{\text{fus},i}} \right) \quad (11)$$

where $\Delta H_{\text{fus},i}$ is the molar enthalpy of fusion of the component i at the melting temperature $T_{\text{fus},i}$; x_i is the mole fraction of component i ; and $T_{\text{fus},i}$ is the melting temperature of component i .

The phase diagrams of the solid dispersion and the mixtures of PEG 6000 with griseofulvin are almost identical. This indicates that the two systems do not differ significantly. The shape of the two experimental phase diagrams characterizes monotectic systems. In such systems the melting temperature of the component melting at a lower temperature remains constant over the whole concentration range. The experimental phase diagrams do not allow the exclusion of the existence of a solid solution or an amorphous distribution of griseofulvin in PEG 6000 at griseofulvin concentrations lower than 5 %. In contrast to the PEG 8000 + griseofulvin phase diagram studied by Law et al.,²⁴ the liquidus line determined experimentally differs significantly from the line calculated by means of eq 11.

The crystalline compounds were characterized by X-ray spectra. The formation of a solid solution of griseofulvin in PEG 6000 reduces the intensity of the characteristic griseofulvin peaks and also increases diffuse scattering. A typical X-ray diffraction pattern for griseofulvin is shown in Figure 11 with the diffraction angles summarized in Table 7.

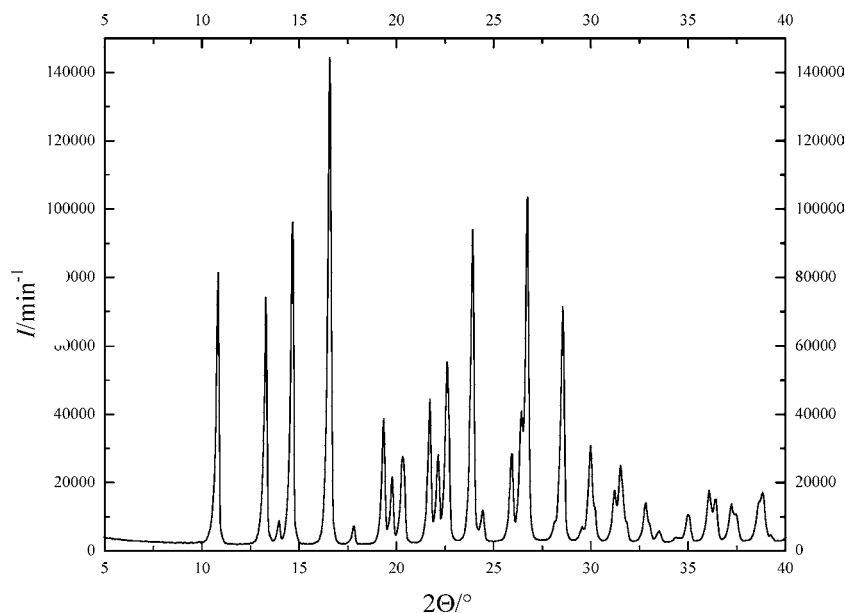
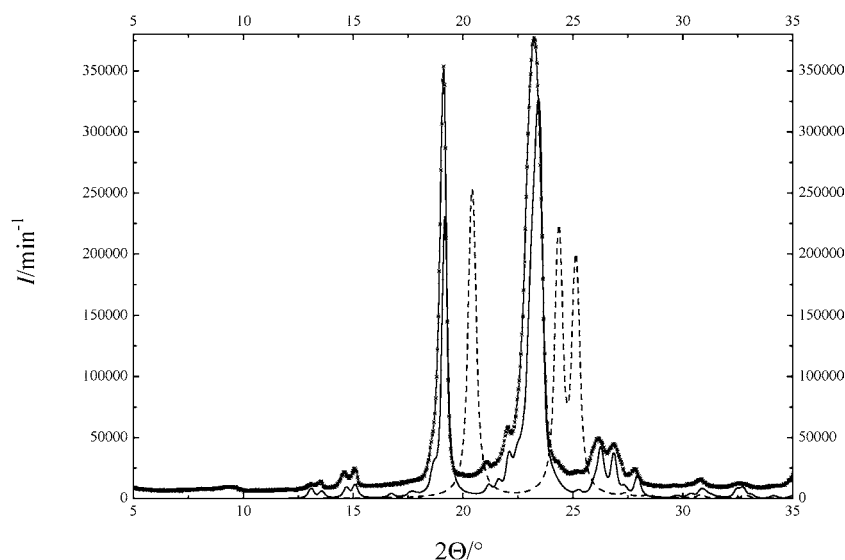
**Figure 11.** X-ray diffraction count intensity I as a function of angle Θ for griseofulvin.**Figure 12.** X-ray diffraction count intensity I as a function of angle Θ for PEG 6000. ---, zigzag calculation; —, 7_2 -helix calculation; -×- thermally untreated.

Table 7. Characteristic Diffraction Angles for Griseofulvin

$2\Theta/^\circ$	$2\Theta/^\circ$
10.82	23.90
13.26	24.42
13.94	25.92
14.64	26.42
16.54	26.72
17.80	28.54
19.34	29.54
19.76	29.98
20.32	31.20
21.70	31.50
21.14	32.80
22.58	33.48

To determine the structure of the PEG used in our studies, X-ray diffraction patterns were taken from thermally treated and untreated polymer. These patterns were compared with diffraction patterns as calculated by means of the program Powdercell 1.0⁹ assuming a zigzag and a 7_2 -helix structure, shown in Figures 12 and 13.

The coordinates used for the calculations of these structures were taken from Takahashi.^{25,26} As can be seen from Figure 12, the PEG used in our experiments shows a 7_2 -helical structure. The relatively high noise is due to a small number of polymer chains remaining in an amorphous state. As Figure 13 shows, there is no structural difference between the thermally

Table 8. Characteristic Diffraction Angles of Thermally Treated and Untreated PEG 6000 Compared with the Diffraction Angles Calculated Assuming a 7_2 -Helix Structure

Nr.	7_2 -helix angle (2Θ)	PEG 6000 treated angle (2Θ)	PEG 6000 untreated angle (2Θ)
1	13.08	13.12	13.08
2	13.56	13.56	13.56
3	14.72	14.64	14.60
4	15.08	15.12	15.08
5	19.16	19.16	19.12
6	21.20	21.08	21.12
7	22.12	22.08	22.04
8	23.44	23.24	23.24
9	26.28	26.20	26.16
10	26.88	26.88	26.88
11	27.96	27.80	27.76
12	30.88	30.84	30.88

treated and the untreated PEG 6000. This impression is confirmed by the diffraction angles given in Table 8.

In both cases, the polymer exists in the form of a 7_2 -helix. In the diffraction pattern of the solid dispersion, the characteristic peaks of griseofulvin at 13.96°, 14.64°, 16.54°, and 17.80° can clearly be assigned to griseofulvin, whereas the peaks at 19.96° and 23.24° are characteristic for PEG 6000; see Figure 14. As these characteristic reflection angles are unchanged, structural changes of griseofulvin as well as of PEG 6000 can be excluded. By means of an external standard, the extent of crystallinity of

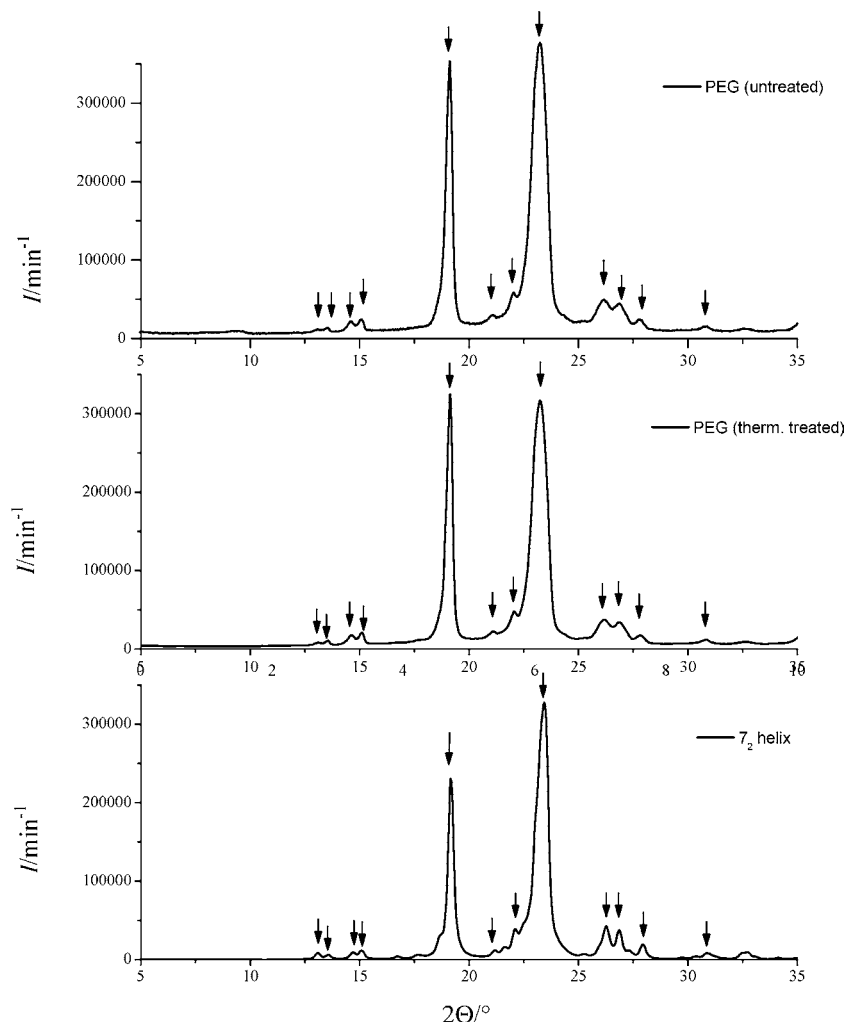


Figure 13. X-ray diffraction count intensity I as a function of angle Θ . Top: thermally untreated PEG 6000. Middle: thermally treated PEG 6000. Bottom: calculated for a 7_2 -helical structure.

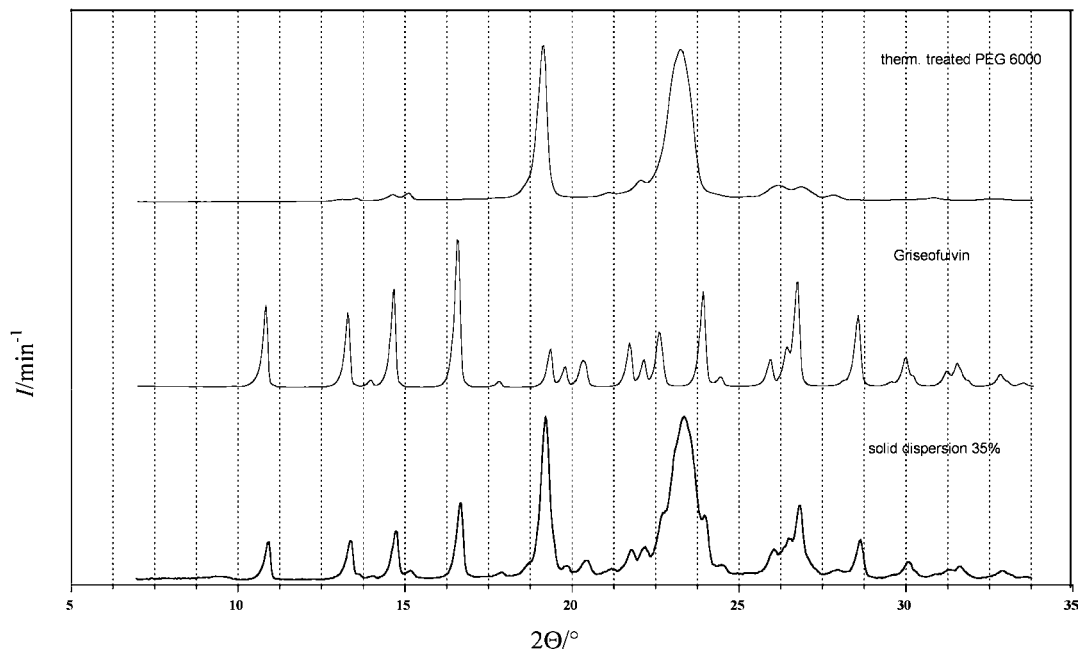


Figure 14. X-ray diffraction count intensity I as a function of angle Θ . Top: thermally treated PEG 6000. Middle: griseofulvin. Bottom: solid dispersion containing mass fraction of 0.35 of griseofulvin in PEG 6000.

griseofulvin in the solid dispersion can be determined to be 0.96 ± 0.09 . The X-ray diffraction patterns of a solid dispersion containing 10 % griseofulvin are shown in Figure 15 along with the characteristic peaks for both griseofulvin and PEG 6000. For griseofulvin, an extent of crystallinity of 0.9 ± 0.2 was determined.

These crystallographic findings are in good agreement with the information obtained from the phase diagrams. In solid PEG containing a mass fraction of griseofulvin less than 0.05, calorimetry could not be used. The diffraction patterns of solid dispersions of PEG 6000 with (1, 2, and 3) % griseofulvin are, not surprisingly, dominated by that of PEG 6000, while fortunately the characteristic peaks of griseofulvin at angles of 10.8° , 13.26° , 14.63° , and 16.58° can be observed as shown in Figure 16.

At these concentrations, the solid dispersions of griseofulvin exist in crystalline form, as listed in Table 9, and do not form solid solutions.

The enthalpy of fusion for an ideal mixture, as which griseofulvin + PEG 6000 can be considered, is given by the sum of the enthalpies of melting for the components²⁰

$$\Delta H_{\text{fus},id} = x_1 \Delta H_{\text{fus},1} + x_2 \Delta H_{\text{fus},2} \quad (12)$$

where x_i is the mole fraction of component i ; $\Delta H_{\text{fus},id}$ is the enthalpy of fusion for griseofulvin + PEG 6000; and $\Delta H_{\text{fus},i}$ is the enthalpy of fusion for component i .

As Figure 17 shows, the enthalpies of fusion are the same as those for solid dispersions of griseofulvin + PEG 6000. Both are identical with the results obtained from eq 12 for various

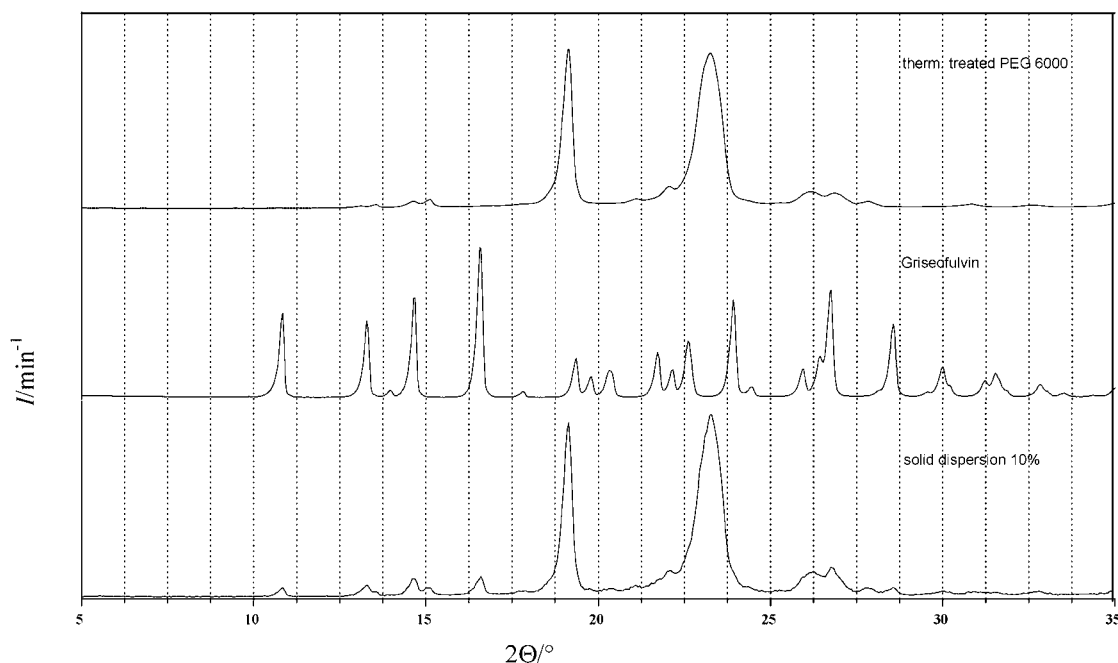


Figure 15. X-ray diffraction count intensity I as a function of angle Θ . Top: thermally treated PEG 6000. Middle: griseofulvin. Bottom: solid dispersion containing mass fraction of 0.10 of griseofulvin in PEG 6000.

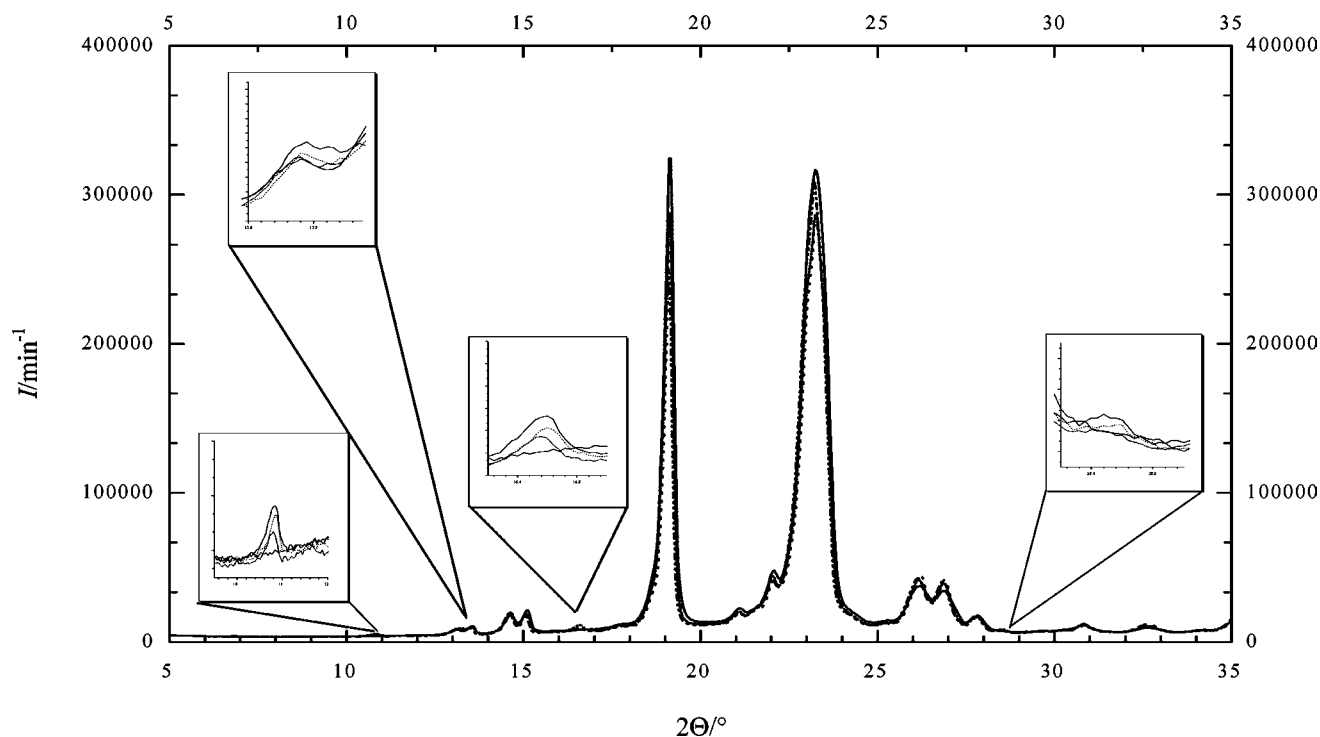


Figure 16. X-ray diffraction count intensity I as a function of angle Θ . — — —, thermally treated PEG 6000; - · - · - ·, solid dispersions containing mass fraction of 0.01 griseofulvin in PEG 6000; · · · · ·, solid dispersions containing mass fraction of 0.02 griseofulvin in PEG 6000; and · · · · ·, solid dispersions containing mass fraction of 0.03 griseofulvin in PEG 6000.

Table 9. Extent of Crystallinity in Solid Dispersions of PEG 6000 Containing Mass Fractions w of 0.01, 0.02, and 0.03 of Griseofulvin along with the Experimentally Determined Mass Fraction w (expt) and Extent of Crystallinity

w	$w(\text{expt})$	extent of crystallinity
0.03	0.03 ± 0.01	0.9 ± 0.4
0.02	0.018 ± 0.007	0.9 ± 0.4
0.01	0.016 ± 0.008	1.5 ± 0.8

mole fractions of griseofulvin. These findings support the concept that griseofulvin does not form solid solutions in PEG 6000.

The solubility of aqueous solutions of griseofulvin in PEG 6000, in view of the findings reported above, hypothesized that the improvement solubility of griseofulvin observed with solid dispersions in PEG 6000 might arise from a simple improvement of the solvent properties of water by the presence of PEG 6000.

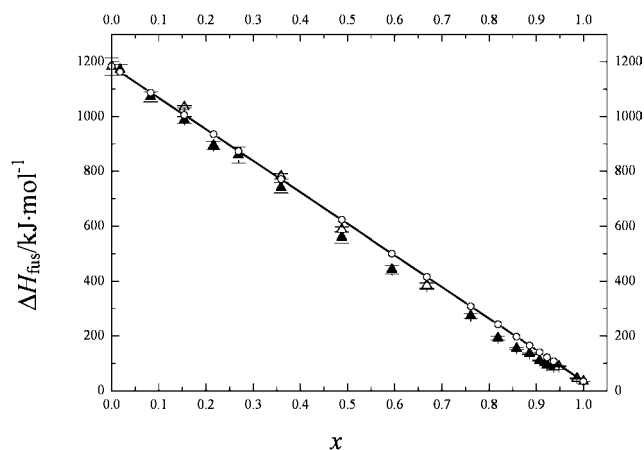


Figure 17. Enthalpy of fusion ΔH_{fus} as a function of the mole fraction x of griseofulvin in PEG 6000. \blacktriangle , solid dispersion; \triangle , physical mixture; \circ , ideal system.

Table 10. Solubility of Griseofulvin in Aqueous Solutions Containing Various Amounts of PEG 6000 at $t = 22^\circ\text{C}$

mass fraction of PEG 6000	solubility of griseofulvin/mg/100 mL	increase in solubility of griseofulvin/%
0	1.292	100
0.01	1.364	105.6
0.02	1.450	112.2
0.05	1.828	141.5
0.10	1.824	141.2
0.20	3.528	273.1
0.30	5.059	391.6
0.40	7.767	601.2

Therefore, aqueous solutions containing various amounts of PEG 6000 were prepared. The solubilities of griseofulvin in these solutions are listed in Table 10.

The increase of the solubility of griseofulvin with increasing concentrations of PEG 6000 is enormous; see Figure 18.

It can be assumed that parts of the poly(ethane-1,2-diol) chains are able to solvate griseofulvin. If this assumption is correct, then other molar mass PEGs should also improve the solubility of griseofulvin in water.

Table 11 lists the solubilities of griseofulvin in aqueous solutions containing PEG 300 and PEG 2000, and both increase the solubility of griseofulvin in water. Comparison of the results in Tables 10 and 11 suggests the improved solubility increases with decreasing PEG molar mass.

4. Conclusions

When solid dispersions of PEG 6000 and griseofulvin are dissolved in water, the water solubility of griseofulvin increases. Other workers^{27–29} have postulated this arises from the formation of solid solutions of griseofulvin in PEG. The thermodynamic data obtained are consistent with this interpretation. However, as the glass transition temperature of solid PEGs of medium molar mass is below room temperature, for small

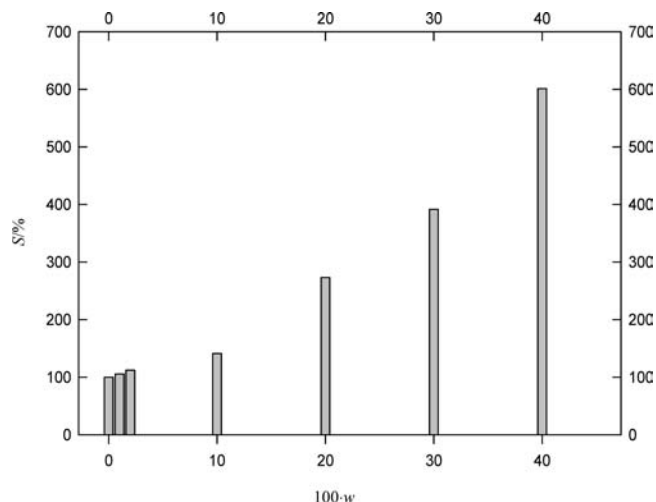


Figure 18. Increase of the solubility S of griseofulvin in aqueous solutions with PEG 6000 as a function of mass fraction of PEG 6000.

Table 11. Solubility of Griseofulvin in Aqueous Solutions of PEG 300 and PEG 2000 at $t = 22\text{ }^{\circ}\text{C}$

PEG mass fraction	solubility of griseofulvin in PEG 300		solubility of griseofulvin in PEG 2000	
	mg/100 mL	%	mg/100 mL	%
pure water	1.292	100	1.292	100
0.01	--	--	1.313	101.6
0.05	1.661	128.6	1.801	139.4
0.10	2.397	185.5	2.379	184.1
0.20	4.354	337.0	4.301	332.9
0.30	9.096	704.0	7.770	601.4
0.40	13.514	1046.0	11.545	893.6

molecules, for example, griseofulvin, diffusion in the polymer is possible. In consequence, solid solutions in PEG are not stable. In solid dispersions prepared by dissolving griseofulvin in a melt of PEG 6000, which was cooled to liquid nitrogen temperatures, fine crystals can be observed under a microscope. As these crystals are smaller than the crystals used for the preparation of mixtures of griseofulvin + PEG 6000, the dissolution rate of the solid dispersion is higher. Similar improvements in the water solubility of griseofulvin can be attained with aqueous solutions of PEG 6000, and improvements of water solubility of griseofulvin are found with aqueous solutions of PEG 300 or PEG 2000.

Literature Cited

- (1) Knoblauch, J.; Zimmermann, I. Thermochemical analysis of the dissolution process of Griseofulvin. *Eur. J. Pharmaceutics Biopharm.* **2007**, *67*, 743–751.
- (2) Hess, H. in: Kortüm, G.; Lachmann, H. *Einführung in die chemische Thermodynamik*, 7; Aufl., Verlag Chemie: Weinheim, 1981.
- (3) Reich, R. *Thermodynamik*; zweite Aufl., VCH: Weinheim, 1993.
- (4) Hemminger, W. F.; Cammenga, H. K. *Methoden der thermischen Analyse*; Springer-Verlag: Heidelberg, 1989.
- (5) Wedler, G. *Lehrbuch der Physikalischen Chemie*; zweite Aufl., VCH Verlagsgesellschaft mbH: Weinheim, 1985.
- (6) Setaram Groupe, *Data processing; A/14Nesofta; A/21 Nesofta; A/34Nesofta; B/18Nesofta*, 1995.
- (7) Weast, R. C. *Handbook of chemistry and physics* - 58 ed.; CRC Press London 1977/78.
- (8) Sabbah, R.; Le Duc, T. H. Étude thermodynamique des trois isomères de l'acide hydroxybenzoïque. *Can. J. Chem.* **1993**, *71*, 1378–1383.
- (9) Kraus, W.; Nolze, G. *Bundesanstalt für Materialforschung*, Rudower Chaussee 5, 12489 Berlin, 1995.
- (10) Jenkins, R.; Snyder, R. L. *Introduction to X-ray powder diffractometry*; J. Wiley: New York, 1996.
- (11) Kirschner, H. *Einführung in die Röntgendiffraktometrie*; Vieweg-Verlag: Braunschweig, 1980.
- (12) Wilson, A. J. C. *International tables for Crystallography*; Kluwer Academic Publishers: Dordrecht, 1992; Vol. C.
- (13) Buckley, C. P.; Kovacs, A. J. Melting behaviour of low molecular weight poly(ethylene oxide) fractions, folded chain crystals. *Colloid Polym. Sci.* **1976**, *254*, 695–715.
- (14) Craig, D. Q. M.; Newton, J. M. Characterization of polyethylene glycols using differential scanning calorimetry. *Int. J. Pharm.* **1991**, *74*, 33–41.
- (15) Craig, D. Q. M.; Newton, J. M. Characterisation of polyethylene glycols using solution calorimetry. *Int. J. Pharm.* **1991**, *74*, 43–48.
- (16) Mathot, V. B. F. *Calorimetry and thermal analysis of polymers*; Hanser Publishers: Munich, Vienna, NY, 1993.
- (17) Wang, G.; Harrison, I. R. Polymer melting: heating rate effects on DSC melting peaks. *Thermochim. Acta* **1994**, *231*, 203–213.
- (18) Yang, R.; Yang, X. R.; Evans, D. F.; Henrickson, W. A.; Baner, J. J. Scanning tunnelling microscopy images of poly(ethylene oxide) polymers, evidence for helical and superhelical structures. *J. Phys. Chem.* **1990**, *94*, 6123–6125.
- (19) Lheritier, J.; Chauvet, A.; Masse, J. Étude des interactions SR 33557/PEG 6000. *Thermochim. Acta* **1994**, *241*, 157–169.
- (20) Atkins, P. W. *Physikalische Chemie*; VCH Verlagsgesellschaft mbH: Weinheim, 1990.
- (21) Wade, A.; Weller, P. J., Eds. *Handbook of Pharmaceutical Excipients*; American Pharmaceutical Association: Washington; The Pharmaceutical Press, London, 2nd ed., 1994.
- (22) Junginger, H. Untersuchungen und Sprüheinbettung von schwer wasserlöslichen Arzneistoffen in Polymere, 4. Mitteilung, Teil 1. *Pharm. Ind.* **1977**, *39* (4), 383–388.
- (23) Kaur, R.; Grant, D. J. W.; Eaves, T. Comparison of Polyethylene Glycol and Polyoxyethylene Stearate as excipients for solid dispersion systems of Griseofulvin and Tolbutamide, I-Phase equilibria. *J. Pharm. Sci.* **1980**, *69*, 1317–1321.
- (24) Law, D.; Wang, W.; Schmitt, E. A.; Long, M. A. Prediction of Poly(Ethylene)Glycol-Drug eutectic compositions using an index based on the van't Hoff equation. *Pharm. Res.* **2002**, *19*, 315–321.
- (25) Takahashi, Y.; Sumita, I.; Tadokora, H. Structural studies of Polyethers IX. Planar Zigzag modification of Poly(ethylene oxide). *J. Polym. Sci.* **1973**, *11*, 2113–2122.
- (26) Takahashi, Y.; Tadokoro, H. Structural studies of Polyethers $-(\text{CH}_2)_m\text{-O-})_n$. X. Crystal structure of Poly(ethylene oxide)-. *Macromolecules* **1973**, *6*, 672–675.
- (27) Wulff, M.; Aldén, M. Phase equilibria in drug-polymer-surfactant systems. *Thermochim. Acta* **1995**, *256*, 151–165.
- (28) Aldén, M.; Wulff, M.; Herdinius, S. Influence of selected variables on heat of fusion determinations by oscillating DSC. *Thermochim. Acta* **1995**, *265*, 89–102.
- (29) Stachurek, I.; Pielichowski, K. Preparation and thermal characterization of Poly(ethylene oxide)/Griseofulvin solid dispersions for biomedical applications. *J. Appl. Polym. Sci.* **2009**, *111*, 1690–1696.

Received for review July 27, 2009. Accepted January 8, 2010.

JE900639J